

Advanced Experimenting on Wave Interaction with Low-Crested Breakwaters

**Ana C. Neves¹, Fernando Veloso Gomes²,
Francisco Taveira Pinto³**

¹University Fernando Pessoa, Faculdade de Ciência e Tecnologia, Praça 9 de Abril, 349, 4249-004 Porto, Portugal, avneves@ufp.edu.pt

²Institute of Hydraulics and Water Research, FEUP, vgomes@fe.up.pt

³Institute of Hydraulics and Water Research, FEUP, fpinto@fe.up.pt

ABSTRACT

Two-dimensional scaled physical tests were carried out in the Hydraulics Laboratory wave tank of the University of Porto in order to more accurately understand the effect of submerged breakwaters on wave-induced velocities and pressure fields. The slow-varying pressures acting normally on the slope were simultaneously measured with the flow-induced velocities at the surface, and an analysis of their distribution along the whole structure-on the front slopes, rear slopes and along the crown-was done as this information is considered potentially useful for hydraulic design. Different points on the breakwater model were considered and diverse wave conditions were tested, allowing study of the dependency of pressures/velocities on model characteristics. Maximum, minimum and mean phase-averaged values of these variables were calculated, allowing the detection of potentially sensitive areas in terms of pressure and velocities at the surface. A spectral analysis of these physical variables was also performed in order to check the results obtained with the regular wave tests.

1. INTRODUCTION

Due to human intervention and natural processes erosion is affecting coasts all over the world. For that reason coastal works are needed, and submerged breakwaters offer part of the solution since they act as a barrier to the coastline, decreasing the direct wave action on the coast and thus the risk of erosion. In this case, environmental and aesthetic impacts are minimized when compared with the use of conventional emerged detached breakwaters, since they are constructed with low crest levels which allow overtopping and some water/sediment circulation along the shoreline. They are also less submitted to wave action (due to their lower height) and therefore the volume of material needed for their construction is smaller than for equivalent emerged structures.

Several authors have conducted studies in order to more accurately understand the behaviour of submerged breakwaters, the complex wave-structure interactions and particularly the wave-induced velocities and pressures applied to these structure.

Yagci *et al.*, 2006, performed an experimental study on dynamic pressures and water velocities on a piled wavescreen. The authors found that there was an exponential decay of the magnitude of dynamic wave pressures with depth. This relation got weaker when it approached the still water level (SWL) due to the nature of the logarithmic function. In-line dynamic wave forces (obtained by summing the in-line dynamic wave pressure components around the cylinder) were found to have similar behaviour, also showing exponential decay.

Tirindelli and Lamberti, 2004, studied wave-induced forces on structural elements of low-crested structures (LCS). From the measurement of velocities in the proximity of the stones and using Morrison-type equations, they calculated the wave forces on rubble mound armour stones and determined the spatial distribution of wave loading along the structure. They pointed out the importance of knowing the velocity and acceleration of the water particles in proximity of the blocks, from which the wave-induced forces applied to the armour layer are determined. In terms of the translational stability of the rocks the authors also focused on the importance of forces parallel to the main flow (parallel to the front and rear slopes and horizontal above the crown). The results show that the most critical location is the seaward crown edge of the structure around the SWL. A decreasing trend of dimensionless peak force parallel to the front slope with a dimensionless vertical distance of the rock from the SWL (water depth/significant wave height) was also confirmed, which means that the highest forces occur on rocks located close to the SWL.

The wave velocity fields in the vicinity of several submerged breakwater models were studied by Taveira-Pinto, 2001, where high velocities were found to occur over the crown in some instants, due to the concentration of wave energy in a reduced water depth. There were moments where an inversion of the flow in the foreshore slope occurred and vertical velocities were significant, resulting in the formation of vortices cells that interfered with the water surface. The transmitted zone of the breakwater was found to be of high turbulence intensity, due to the expansion of the flow section and the energy dissipation.

Neves *et al.*, 2006 also analysed the velocity field in the vicinity of two breakwater models through experimental measurement results. The area located in the leeward upper part of the structure was identified as potentially critical area, where the maximum and minimum velocities were registered. The crown of the structure (namely its edges) was also suggested to be potentially sensitive area, as large dynamic pressures and velocities at the surface occur in this section.

Bleck & Oumeraci, 2001, 2002, Yamashiro *et al.*, 2000 and Taveira & Neves, 2005 analysed the water surface elevation spectra around submerged breakwaters. Among other conclusions, it was found that there are important differences between the spectrum forms of water surface elevation of seaward and leeward points on the structure. A decrease in the total wave energy and a broadening of the spectrum behind the structure was also found, although no change of the peak period was observed (the highest energy remained at the same frequency).

Although former studies provided a useful information base, it was believed that a greater understanding of wave-induced pressures and velocities acting at the surface of submerged breakwaters was still needed.

2. WAVE PRESSURES

An accurate estimation of the hydraulic pressures/loads due to wave action on the elements of a submerged breakwater provides useful information to the design criteria. Although much is already known about the stability of these structures, a detailed description of the magnitudes and of the physical phenomena of wave-induced pressures applied to the structures, and namely to the individual units of structures, is still necessary.

The interaction of wave action on coastal structures, depending on the characteristics of the sea conditions to which they are exposed, can generate pressures composed of two components: pulsating and impulsive. The impulsive pressures are localized in time and space and have a very high magnitude and a very short rise and fall time. Though they may be dangerous for breakage of fragile concrete armour units or local yielding, the impulsive

nature of these impacts prevents them from being dangerous to the overall stability of armour units, so they are of less interest to the designer, Tirindelli and Lamberti, 2004. They are of great interest for monolithic and massive structures, Alderson *et al.*, 2006. Pulsating pressures on the other hand, are slow-varying pressures which, from the standpoint of a design engineer, can be more critical than impulsive ones as they transfer high momentum to structural elements. The impulsive type pressures require high sampling rates but pulsating ones can be captured by smaller data sampling rates.

The objective of this study was primarily concerned with slow-varying pressures since, as previously mentioned, they constitute the main potential risk for the stability of rubble-mound structures.

Considering linear wave theory and sinusoidal waves and setting the atmospheric pressure equal to zero, the vertical distribution of pressure is conventionally written as

$$p(z, t) = \rho g K_p(z) \eta + \rho g z \quad (1)$$

where p represents the total pressure, ρ is the water density, g the gravitational acceleration, z is the vertical position, t is the time, η is the instantaneous surface elevation and $K_p(z)$ is the pressure response factor.

K_p varies with z as a hyperbolic cosine ($K_p = 1$ at $z = 0$) and is defined as,

$$K_p(z) = \frac{\cosh[k(d + z)]}{\cosh kd} \quad (2)$$

where k represents the wave number, equal to $2\pi/L$, and d is the water depth.

The hydrostatic pressure in the absence of the waves is given by $\rho g z$, with $p = 0$ at the free surface ($z = 0$). $K_p(z) \rho g \eta(t)$ is the wave-induced pressure, also designated as dynamic pressure. This dynamic pressure is the contribution of two factors: the surcharge of pressure caused by the free surface displacement, and the vertical acceleration of the fluid particles.

3. EXPERIMENTAL SET-UP

The experiments were carried out in the wave tank of the Faculty of Engineering of the University of Porto (FEUP). The wave tank is 12 m wide, 28 m long, and has a maximum water depth of 1 m, Figure 1.

The piling up of water due to return (offshore directed) flow over the model can affect



Figure 1 Wave tank ($28 \times 12 \times 1 \text{ m}^3$) of the Hydraulics Laboratory of FEUP.



Figure 2 Rough impermeable model.

measurements in the leeward part of the structure. This was prevented in the present experimental set-up configuration by allowing the wave-induced currents to return through the channel. For that reason the measurements on the leeward of the structure were considered to be more reliable, Losada *et al.*, 2005, Cox & Tajziehchi, 2005.

Three different models were tested, all having a similar cross-section but different roughness and permeability characteristics: a smooth and a rough impermeable model and a rough permeable one.

The smooth impermeable model was constructed using a perspex structure and the rough one used a similar structure with smaller dimensions and stones glued to its surface, simulating the armor block. The armour layer stones had $D_{n50} = 4.4$ cm and in Figure 2 it is represented the rough impermeable model.

The rough permeable model was constructed in situ, with a permeable core and a stone armour layer $2D_{n50}$ wide. Figure 3 shows the rough permeable model located in the measuring section.

The three models had a crest width of 0.30 m, a height of 0.40 m and 1:1 slopes and were constructed using a 1/40 Froude scale.

In total, twenty-seven points along the model were considered, where velocity at the surface and total pressure were simultaneously calculated. The water surface elevation was registered with capacitance wave probes located in the same vertical alignment in order to

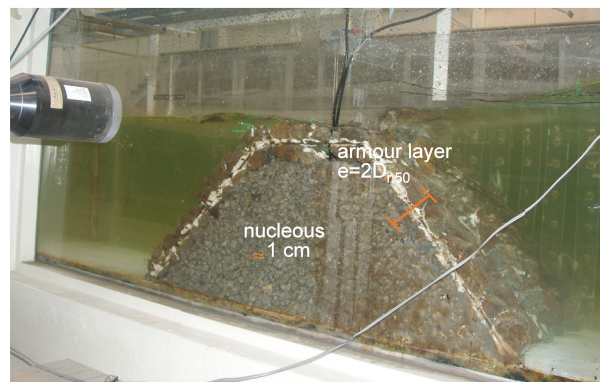


Figure 3 Rough permeable model.

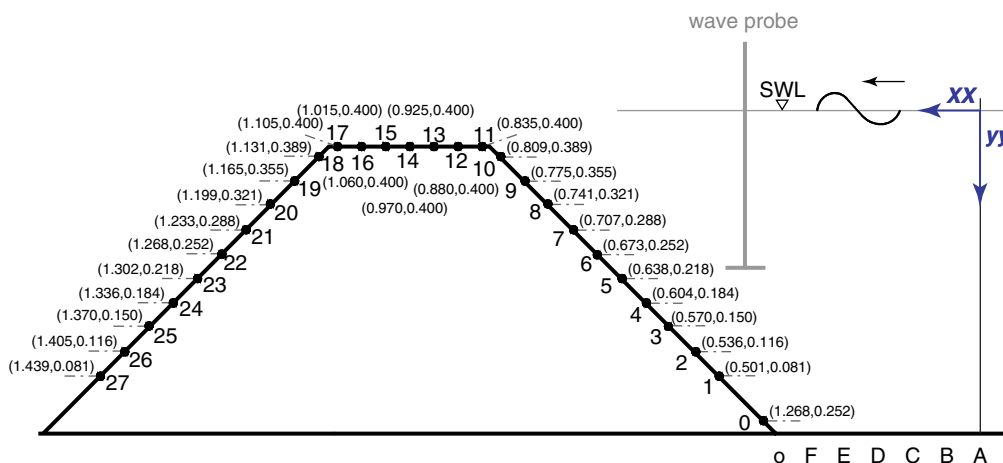


Figure 4 Location of the measuring points.

synchronise the wave phases. The location of the measured points is shown in Figure 4.

The origins of vertical and horizontal axes were considered to be in the bottom of the tank and in 0.42 m seaward of the model and, respectively. The exact location of the measured points is indicated in Table 1.

The pressure measurements were made using Druck miniature, model PDCR 35/D pressure sensors, and the velocities at the surface (in the direction of the slope) were measured using a Laser Doppler velocimeter. A 2-watt Argon-Ion Laser working in “single mode” and a Dantec system with an optic fiber of one component provided the velocity data.

The signal processing was done using a Burst Spectrum Analyzer, which allowed the simultaneous acquisition of the Doppler and of the analogical signals in a way that each validated velocity count corresponded to a pressure and a water surface elevation value.

Both analogical signals were recorded at a 200 Hz data rate and the velocity data rate

Table 1 Coordinates of the measuring points

Point	x (m)	z (m)	Point	x (m)	z (m)
P1	0.501	0.081	P2	0.536	0.116
P3	0.570	0.150	P4	0.604	0.184
P5	0.638	0.218	P6	0.673	0.252
P7	0.707	0.287	P8	0.741	0.321
P9	0.775	0.355	P10	0.809	0.389
P11	0.835	0.40	P12	0.880	0.40
P13	0.925	0.40	P14	0.970	0.40
P15	1.015	0.40	P16	1.060	0.40
P17	1.105	0.40	P18	1.131	0.389
P19	1.165	0.355	P20	1.199	0.321
P21	1.233	0.287	P22	1.268	0.252
P23	1.302	0.218	P24	1.336	0.184
P25	1.370	0.150	P26	1.405	0.116
P27	1.439	0.081			

Table 2 Test conditions.

Water depth (m)	0.45
Incident wave height (m)	0.05, 0.065, 0.075, 0.15
Incident wave period (s)	1.5

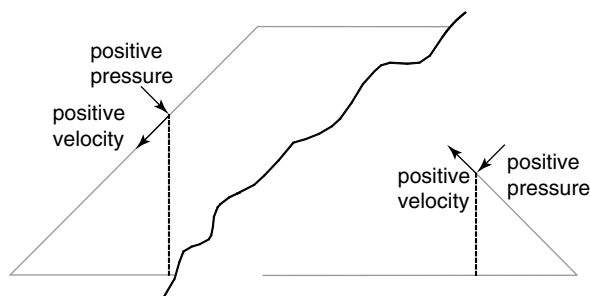


Figure 5 Adopted positive convention.

ranged between 20 and 100 Hz, depending on the magnitude of the velocities being measured and, consequently, on the location of the measuring point.

The same wave conditions were used in tests performed with the three models in order to analyze the effect of roughness and permeability of the structures on the wave-induced pressure/velocity field.

Table 2 presents the tests conditions used during the experiments with regular waves.

Tests with irregular waves were also performed for the respective incident significant wave heights and peak frequencies.

Figure 5 represents the adopted convention for the positive pressure acting on the model and the positive shear velocity.

4. RESULTS AND DISCUSSION

The raw data were analysed and mean and root mean square values were calculated for 50 different wave phase instants. Figure 6 illustrates some of the raw dynamic pressure registered, and Figure 7 shows the respective mean and mean square values of this variable. These values are in relation to the smooth impermeable model for tests performed with a wave height equal to 0.065 m and a wave period equal to 1.5 s.

From the results it can be seen that wave-induced dynamic pressure grows with the distance to the bottom. The highest maximum dynamic pressures were observed in the upper region of the model slope, which could indicate a potentially sensitive area. Interestingly, it was also found that the wave-induced dynamic pressure in the point P1 was considerably higher than the one found in the point located immediately above (which is frequently related with scour at the toe of the breakwater).

Figures 8 and 9 represent some of the results obtained for four different sections of the breakwater models. Points P1 and P5 in the seaward slope and P23 and P27 in the leeward slope of the model show differences in dynamic pressure and velocities at the surface for the tested wave conditions.

A comparison between the values found in leeward (P23 and P27) and seaward slopes (P1 and P5) shows a great attenuation, as a result of wave dissipation and breaking over the structure. The permeable model presents much lower values than the two impermeable

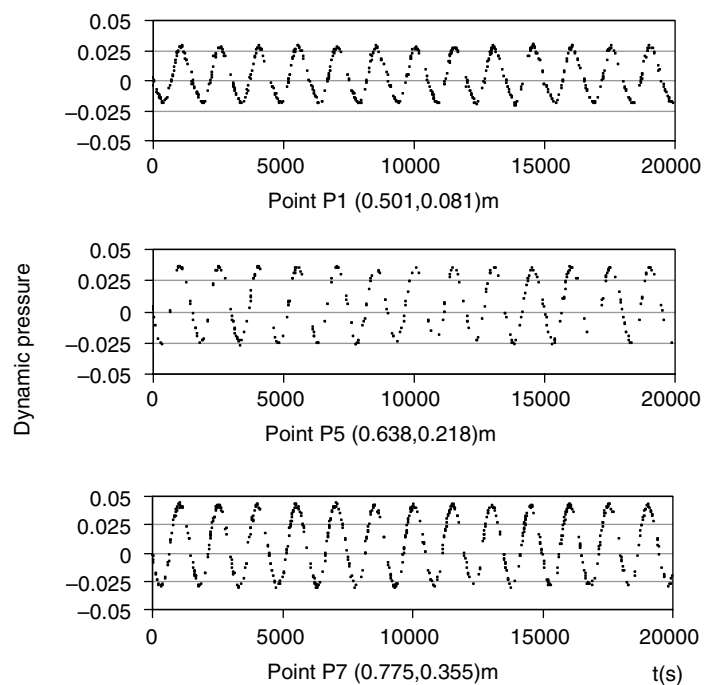


Figure 6 Dynamic pressure time series ($H_i = 0.065$ m, $T = 1.5$ s, $d = 0.45$ m, smooth impermeable model).

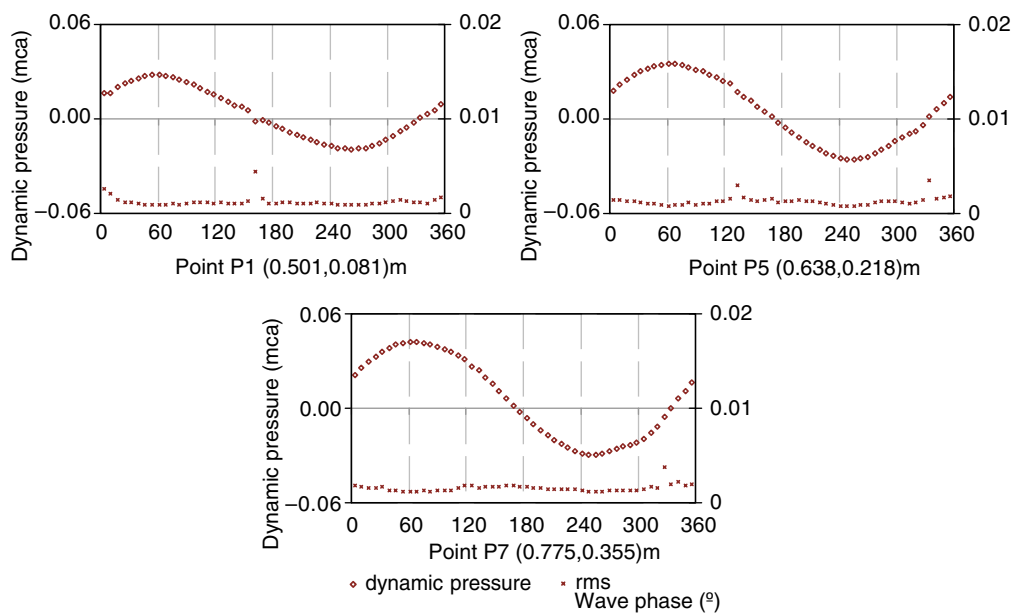


Figure 7 Mean dynamic pressure and root mean square values along the wave phase ($H_i = 0.065$ m, $T = 1.5$ s, $d = 0.45$ m, smooth impermeable model).

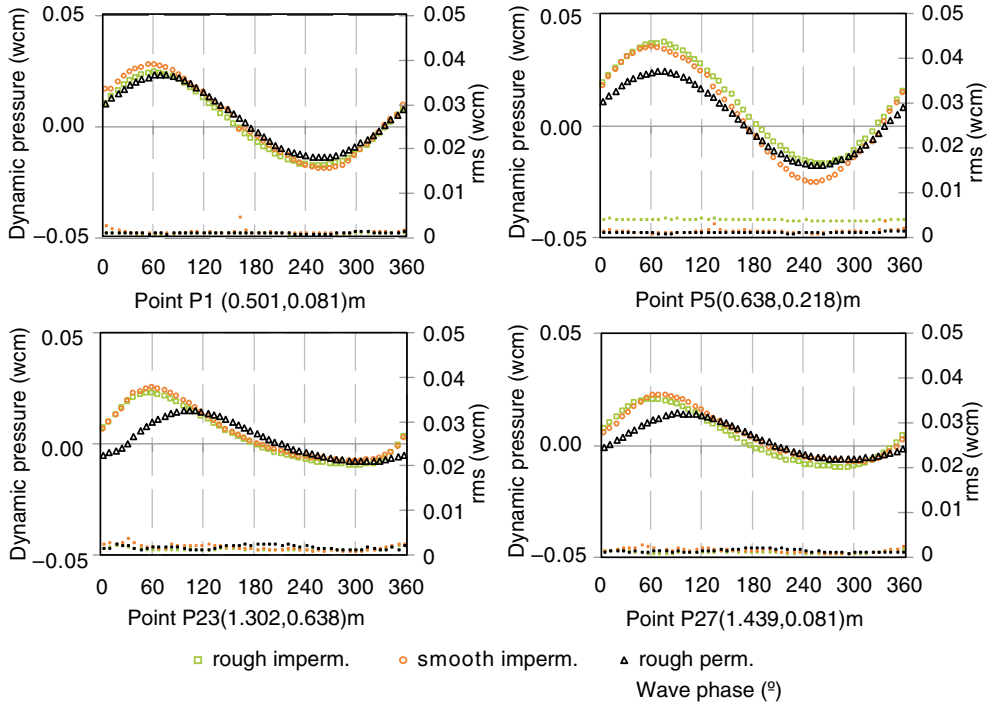


Figure 8 Mean dynamic pressure and root mean square values along the wave phase ($H_i = 0.065$ m, $T = 1.5$ s, $d = 0.45$ m).

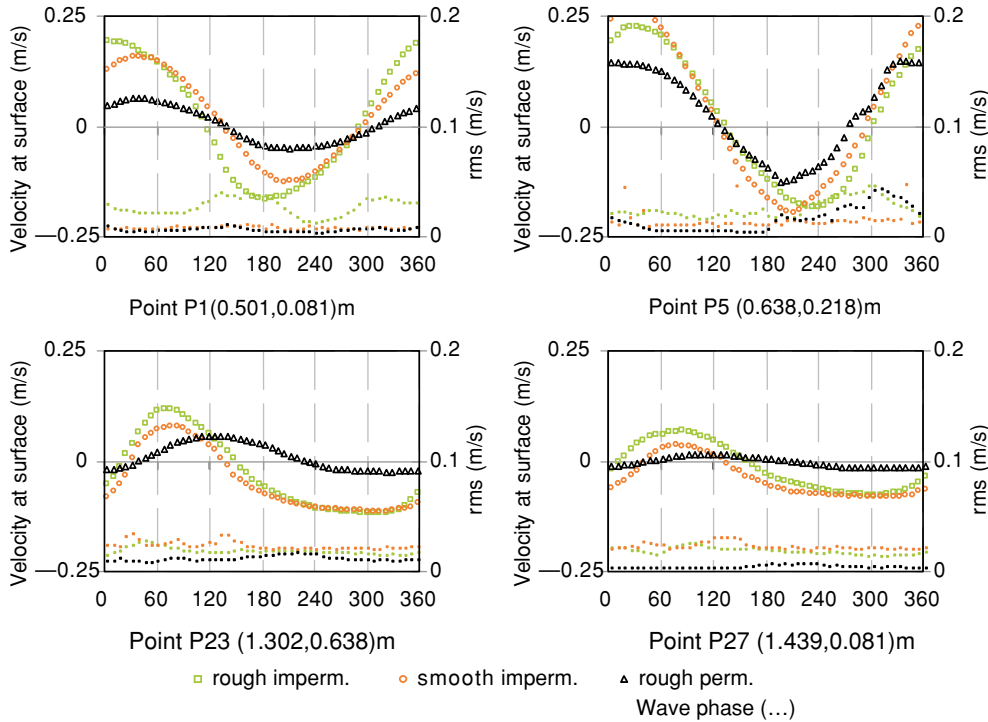


Figure 9 Mean velocity at the surface and root mean square values along the wave phase ($H_i = 0.065$ m, $T = 1.5$ s, $d = 0.45$ m).

models, indicating that permeability significantly affects wave-induced dynamic pressure and velocity at the surface values. Although roughness also has an attenuating effect, this was shown to be much less important than the effect of permeability.

It is interesting that the rough impermeable model showed higher dynamic pressures at the points located on the leeward slope than did the smooth impermeable one. The major differences between rough and smooth model values were observed in the profiles located in the upper area of the breakwater, near the crown (P9 and P19). Point P9, located near the seaward edge of the crown, registered the highest negative velocity and it is interesting to note that for this case the values obtained for the smooth model were almost double those registered in the rough model, again showing the impact of roughness on the dissipation and attenuation of water particle velocities.

The differences between the values of the dynamic pressures in the different models can be explained by the distinct characteristics of the models and their effect on the reflection properties of the structures and in the wave propagation near them, since the dynamic pressure is highly dependent on the water surface elevation.

It was observed that for the same profiles (excluding the ones located in the leeward slope of the model) the variation of dynamic pressure values along the wave phase shows a similar trend to the water surface elevation variation, which could mean that in these locations of the breakwater this surcharge of pressure is mainly caused by the free surface displacement, and vertical acceleration of the fluid particles is not so significant.

The highest positive velocities at the surface were registered in the upper seaward slope and over the crown, indicating that there is a strong onshore directed flow in this area. Point P19, located in the higher part of the leeward slope, also exhibited very high velocities at the surface, indicating that this area must also be considered as a potentially critical area.

In Taveira-Pinto & Neves, 2003, 2006, it was concluded that there was correlation between the wave-induced dynamic pressure and the horizontal component of the velocity, both in progressive and partially standing waves. A preliminary analysis of the correlation between the maximum wave-induced dynamic pressures and the maximum velocities at the surface for each measurement point was performed, and Figure 10 shows the results for each one of the models for one of the wave conditions.

Linear curves were fitted to the data and a preliminary analysis of the results show that maximum dynamic pressures and velocities at the surface show high correlation, with R^2 ranging from 0.75 and 0.80.

Some of the results obtained with the tests performed with irregular waves with incident significant wave height equal to 0.065 m and peak frequency equal to 0.67 Hz and for the same water depth, 0.45 m, are illustrated in Figures 11 to 14. These results respect to tests performed with the rough permeable model.

It can be seen that the spectral density of the total pressure elevation is significantly different in seaward and leeward slopes. The spectral density peak tends to increase at points located in the upper sections of the seaward slope. The same happens at the points located in the leeward slope. Spectra relative to the points located in the leeward slope reveal a smaller second peak, located in the 1.33 Hz frequency (double of the peak frequency) and also higher spectral density at the higher frequencies.

In Bleck & Oumeraci, 2001 it is mentioned that waves behind submerged breakwaters show a decrease in the total energy density spectrum and a deformation of the spectrum (change in the wave form/period) while passing the submerged breakwater. The spectrum behind the structure becomes multi-peaked and broader. As wave-induced pressures are highly dependent on the water surface elevation, these phenomena can be the explanation for

AQ: Please
check -0.05
or -0.5.

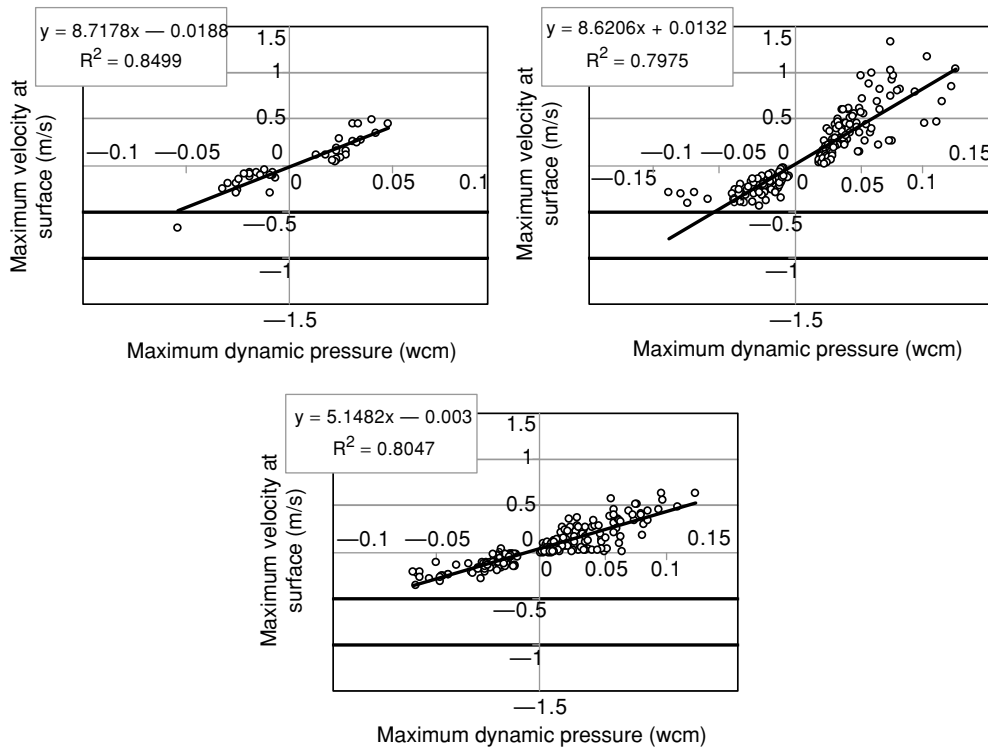


Figure 10 Maximum velocity at the surface and maximum dynamic pressure ($H = 0.065$ m, $T = 1.5$ s, $d = 0.45$ m).

the transformations which occur in the wave-induced pressures spectra.

The spectral density peak of the velocities at the surface of the structure obtained for all the points was registered for the wave peak frequency, and it should be noted that this value is reduced the value from the upper part of the seaward slope to immediately after passing the

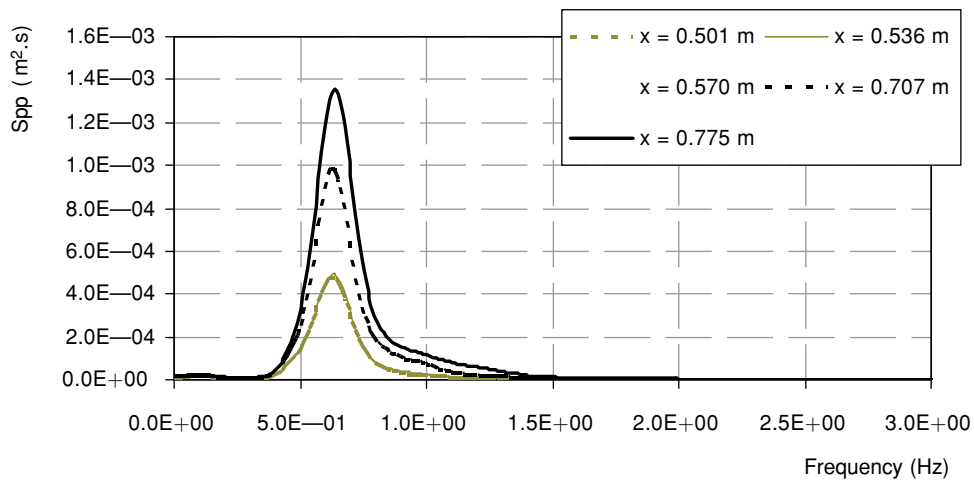


Figure 11 Spectral density of the total pressure (seaward slope, $H_s = 0.065$ m, $f_p = 0.67$ Hz, $d = 0.45$ m, rough permeable model).

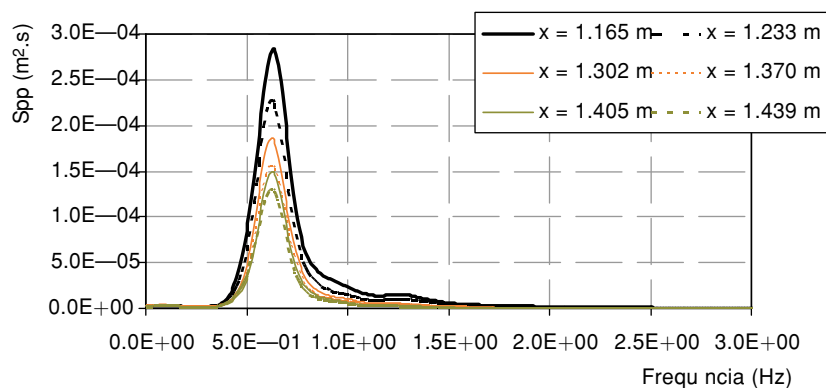


Figure 12 Spectral density of the total pressure (leeward slope, $H_s = 0.065$ m, $f_p = 0.67$ Hz, $d = 0.45$ m, rough permeable model).

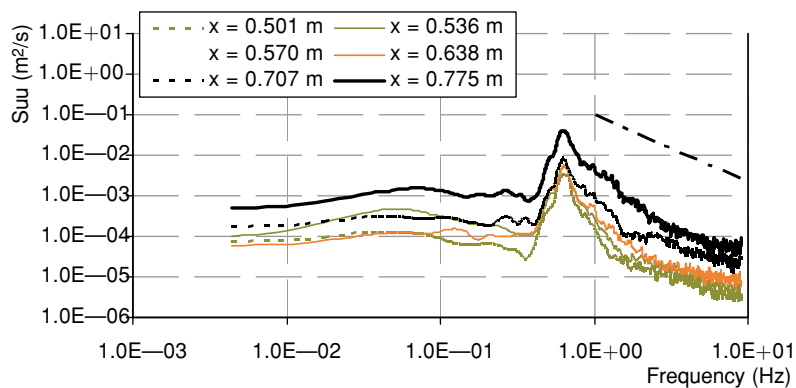


Figure 13 Spectral density of velocities at the surface (seaward slope, $H_s = 0.065$ m, $f_p = 0.67$ Hz, $d = 0.45$ m, rough permeable model).

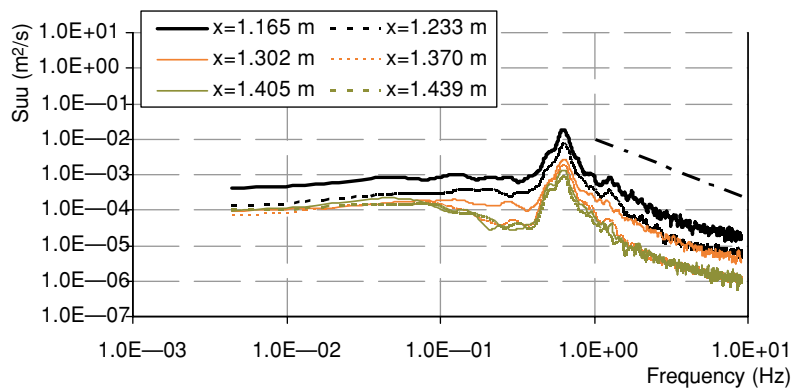


Figure 14 Spectral density of velocities at the surface (leeward slope, $H_s = 0.065$ m, $f_p = 0.67$ Hz, $d = 0.45$ m, rough permeable model).

crown of the structure point is reduced by half).

5. CONCLUSIONS AND FINAL REMARKS

It is evident that determining the pressures and velocities acting on the surface of submerged breakwaters can provide useful information on the stability of the blocks that form this type of structure. These physical variables were simultaneously measured in different sections of three submerged breakwater models with different roughness and permeability characteristics.

The highest dynamic pressures and velocities at the surface were found in the points located seaward, in the upper part of the slope, and over the crown.

It was also proven that roughness, and especially the permeability of these structures, significantly affect the wave-induced pressures and velocities as they have a major influence in the water propagation near them.

The results have proven that wave-induced dynamic pressures are highly dependent on water surface elevation and also exhibited a strong correlation with the velocities at the surface.

The results obtained with irregular wave tests have shown similar behaviour to the ones performed with regular waves.

In future developments it is intended to extend this analysis to other wave conditions.

REFERENCES

- [1] Alderson, J., Allsop, W., Clarke, J., Measurement of Problematic Impulsive Wave Loads on the Underside of an Exposed Jetty, in: Veloso Gomes, F., Taveira Pinto, F. and das Neves, L., ed., *Book of Abstracts of the 1st International Conference on the Application of Physical Modelling to Port and Coastal Protection*, IAHR, Madrid, Spain, 2006, pp. 207-210.
- [2] Bleck, M., Oumeraci, H., Wave Damping and Spectral Evolution at Artificial Reefs, in: Edge, B., Hemsley, M., ed., *Proceedings of the 4th International Symposium on Ocean Wave Measurements and Analysis*, American Society of Civil Engineers, San Francisco, USA, 2001, pp. 1063-1072.
- [3] Cox, R., Tajziehchi, M., 2D Experimental Modelling of Hydrodynamics Effects of Submerged Breakwaters in: Agustin Sanchez-Arcilla, ed., *5th International Conference on Coastal Dynamics 2005*, American Society of Civil Engineers, Barcelona, Spain, 2006.
- [4] Losada, I., Garcia, N., Lara, J., 2005. Report on turbulent flow velocities in the surface region of LCS. *DELOS (Environmental Design of Low Crested Coastal Defence Structures) Project*, Deliverable 23 and 44.
- [5] Neves, A. C., Veloso-Gomes, F., Taveira-Pinto, F., Proença, M. F., 2006. Water Surface Elevations, Velocities and Pressures at Submerged Breakwaters in: Veloso Gomes, F., Taveira Pinto, F. and das Neves, L., ed., *Proceedings of the 1st International Conference on the Application of Physical Modelling to Port and Coastal Protection*, IAHR, Madrid, Spain, 2006, pp. 31-441.
- [6] Taveira-Pinto, F. 2001. *Velocity Fields in the Vicinity of Submerged Breakwaters*, PhD Thesis, Faculty of Engineering of University of Porto, Porto, Portugal (in Portuguese).
- [7] Taveira-Pinto, F., Neves, A. C., (2005). Spectral Analysis of Water Surface Elevations Near Submerged Breakwaters, in: Brebbia, C. A., Cunha, M. C., ed., *Proceedings of the 7th International Conference on Modelling, Measurements, Engineering and the Seas and Coastal Regions - Coastal Engineering 2005*, Wessex Institute of Technology, Algarve, Portugal, pp. 271-280.
- [8] Tirindelli, M., Lamberti, A., 2004. Wave-Induced Forces on Structural and Biotic Elements of Low-Crested Structures, in: Smith, K. M., ed., *Proceedings of the 29th International Conference Coastal Engineering 2004*, World Scientific Pub Co Inc, Lisbon, Portugal, pp. 4228-4239.

- [9] Yagci, O., Kirca, V. S. O., Kabdasli, M. S., Celik, A. O., Unal, N. E., Aydingakko, A., An experimental model application of wavescreeen: dynamic pressure, water particle velocity and wave measurements, *Ocean Engineering* 33 , 2006, pp. 1299-1321.
- [10] Yamashiro et al., 2000, Experimental Study on Wave Field Behind a Submerged Breakwater, in: Losada, ed., *Proceedings of the International Conference Coastal Structures '99*, Balkema, Rotterdam, , PP. 675-682.